Proceedings of the 9th International Conference on Fluid Flow, Heat and Mass Transfer (FFHMT'22)
Niagara Falls, Canada – June 08-10, 2022
Paper No. 122
DOI: 10.11159/ffhmt22.122

Heat Transfer Coefficients in Perforated Fins

Kymani M. Brown, Mohammad Reza Shaeri
Department of Mechanical Engineering, University of the District of Columbia, Washington, DC 20008, USA
kymani.brown@udc.edu; mohammadreza.shaeri@udc.edu

Abstract **–** Three-dimensional steady state and incompressible flow and heat transfer are simulated over a perforated fin to validate the numerical heat transfer coefficients with experimental data. The validated numerical approach is necessary to investigate the complex flow patterns over perforations, which is difficult and costly to capture through experiments. Perforations with square cross sections are distributed equidistantly along the length of the fin. The simulation is performed for a laminar airflow with Reynolds numbers between 992 and 1722. The Navier-Stokes and energy equations are discretized through the finite volume approach, and the pressure and velocity components are coupled by the SIMPLEC algorithm. Excellent agreements (below 6.1%) are obtained by comparing average numerical and experimental Nusselt numbers. Suggestions for future research to address the current gaps in understanding the thermo-fluid mechanism in perforated fins are provided.

Keywords**:** Perforated fin; Heat sink; Nusselt number; Laminar flow; CFD.

1. Introduction

Simplicity, low cost, and ease of maintenance have made air-cooled heat sinks as primary thermal management solutions in a wide range of applications [1]. However, these cooling systems are prone to low thermal performance due to poor thermal properties of the air as the coolant [2]; therefore, leveraging heat transfer enhancement techniques in air-cooled heat sinks is essential to overcome such a drawback. Laterally perforated fins (LPFs) made by implementing perforations on the lateral surface of the fins has been a popular technique for improving heat transfer rate [3]. LPFs potentially enhance heat transfer rate by frequent terminating and restarting the thermal boundary layer before and after perforations, respectively. Besides, because of perforations, perforated fins reduce the weight of cooling systems. Investigating thermo-fluid mechanism in heat sinks made by perforated fins have been the subject of extensive research, particularly a series of research performed by the author in [1], [4], and [5]. However, still knowledge in thermo-fluid phenomena in perforated fins is limited due to lack of understanding the flow patterns over perforations. In the recent research by the author in [4] and [5], thermal performances of LPFs were investigated through detailed experiments and for the first time in the literature, correlations were developed to predict Nusselt numbers in LPFs. Also, it was demonstrated that the heat transfer in LPFs is mainly dictated by the interactions of flow over perforations. However, understanding such a complex flow pattern through experiments will lead to costly research due to requirement to sophisticated visualization tools. Nevertheless, computational fluid dynamics (CFD) can be a reliable tool to address unknown physics in LPFs and, in turn, designing efficient air-cooled heat sinks. To develop an accurate simulation approach, it is necessary to validate the simulation by comparing the computational and experimental data obtained from a LPF rather than a solid fin (i.e., a fin without perforations). In fact, the latter comparison may result in underestimated/overestimated Nusselt numbers in LPFs.

In the present study, heat transfer coefficients of a LPF are obtained through three-dimensional CFD and compared with those of acquired from experiments in the previous research at [4] and [5]. The operating conditions and the design parameters are maintained similar to those in the experimental studies. To the best of the authors' knowledge, the present study is among few attempts in the literature to compare the computational and experimental Nusselt numbers of a given LPF at exactly the same operating conditions and design parameters.

2. Problem Description and Computational Approach

The heat sinks in the experimental studies in [4] and [5] were made of 6063-T5 aluminum alloy and included 19 parallel channels (20 fins) with the fin thickness at 0.96 mm, and the channel length, height, and width at 203 mm, 22.86 mm, and 2.18 mm, respectively. Square cross-sectional perforations at three different perforation sizes and five different

porosities were fabricated on the lateral surfaces of the fins. The porosity was defined as the fraction of void volume of the fins due to perforations, to the volume of the solid fin. A blower circulated ambient air through a duct and heat sinks. The air velocity inside the duct was adjusted by regulating the voltage of a power supply that powered the blower. At the present study, one heat sink from the experimental studies at a porosity of 0.15 and a perforation size (L_P) of 15.24 mm is selected. The porosity of 0.15 corresponds to three perforations, as schematically shown in Fig. 1. The channel length (L), height (H), width (W_{ch}), and the find thickness (t_f) are the same as those in the experiments. The distance from the bottom edge of the perforations to the heat sink base, and that from the top edge of the perforations to the top of heat sink are equal to 3.81 mm.

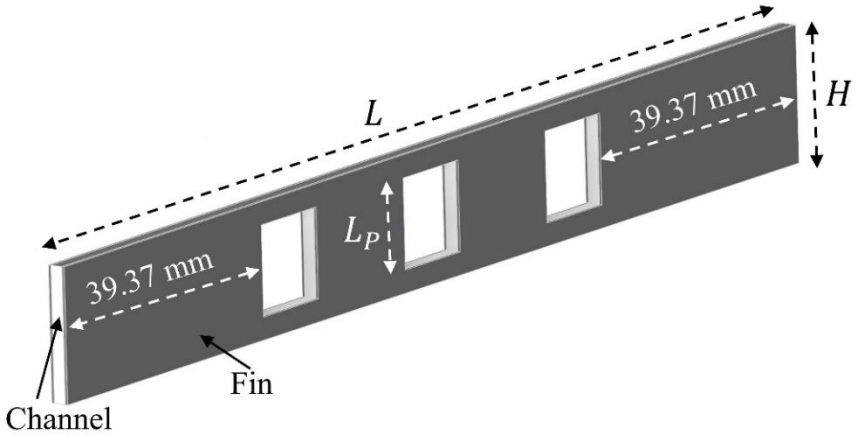

Fig. 1: Schematic of perforated fin in this study.

The experimental Nusselt numbers (Nu_{exp}) in [5] was calculated as below:

$$Nu_{\text{exp}} = \frac{hW_{\text{ch}}}{k_f} = \frac{\left(\frac{Q_{\text{input}}}{N}\right)W_{\text{ch}}}{k_f(2HL)(1-\emptyset)\left(T_{b,\text{avg}} - T_i\right)} \quad (1)$$

where h is the average heat transfer coefficient, k_f is the fluid thermal conductivity, Q_{input} is the total applied heat to the heat sink base, N is the number of channels (19), $\emptyset$ is the porosity (0.15 in this study), $T_{b,\text{avg}}$ is the average channel base temperature, and T_i is the inlet air temperature. The term $(2HL)(1-\emptyset)$ corresponds to the heat transfer area inside the channel. The procedure to calculate Nu_{exp} was based on the method proposed in [6]. In the experiments in [5], the temperature distribution at five different locations across the heat sink base was measured by locating five thermocouples at the base, as shown in Fig. 2(a). A uniform heat load at 100 W (Q_{input}) was applied to the base of the heat sinks using an insulated flexible heater that was adhered to the heat sink base and covered the entire base. The $T_{b,\text{avg}}$ in Eq. (1) was calculated using the assumption of one-dimensional heat diffusion in a distance between the plane of the embedded thermocouple and the channel base, by using the average temperature of five temperatures measured by embedded thermocouples. However, simulation of the entire heat sink requires a large number of grid structures that results in a time-consuming computational analysis. Therefore, due to the symmetry and uniform air flow parallel to the fins, simulations are performed only for one channel and half of each fin instead of array of channel and fins, as shown in Fig. 2(b). In the experiments, the inlet temperature (T_i) was used as the reference temperature (T_{ref}), shown in Fig. 2(b), to calculate the Nusselt numbers. Since only one channel is used for simulation, the $T_{b,\text{avg}}$ obtained from the experiments at an individual Reynolds number is used as the boundary condition for the channel base. The rest of boundary conditions for the simulations are as follows: at the inlet of the channel, an inlet mass flow rate equal to that in the experiments is applied.

For the outlet conditions, zero axial gradients for all the variables are imposed. All other surfaces are walls with no-slip boundary conditions. For obtaining the temperature distribution on the interface of solid and fluid (i.e., inside the channel and perforations), Fourier's heat conduction equation is solved simultaneously with forced convection in the fluid. The heat sink base temperature is fixed at $T_{b,\mathrm{avg}}$, and the remaining walls are adiabatic, similar to the experiments. The inlet temperature is maintained the same as experiments and equal to $T_{\mathrm{i}} = 22℃$. Three-dimensional steady state and incompressible flow and heat transfer are simulated by solving continuity, momentum, and energy equations using Ansys Fluent. The governing equations are discretized through the second order upwind using the finite volume approach. The SIMPLEC algorithm is employed to couple the pressure and velocity components. A grid structure with almost 200,000 elements was selected after reaching an independency between the heat transfer coefficients and the number of computational cells.

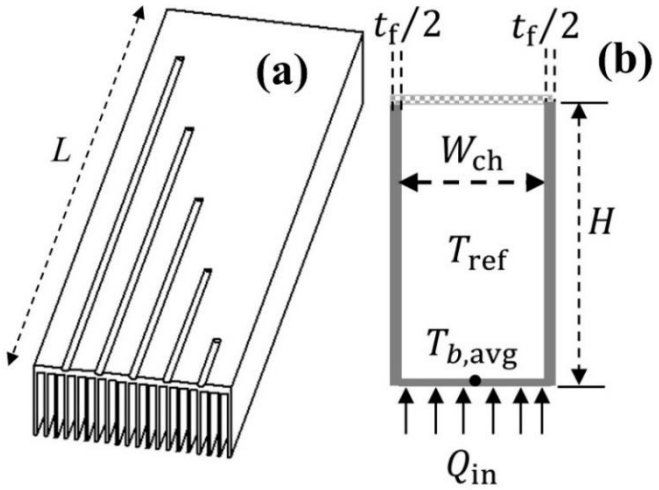

Fig. 2: (a): Schematic of the heat sink base in the experiments in [4] and [5]; (b) Unit cell of a channel used for simulation.

3. Results

The Richardson number (ratio of the Grashof number to the square of Reynolds number) was calculated to assess the impact of natural convection heat transfer. It was demonstrated that the natural convection is negligible due to low Richardson number (below 0.003) [5]. Therefore, the forced convection is the dominant mode of heat transfer in this study. The simulations are performed at different inlet mass flow rate and, in turn, channel Reynolds number (*Re*), described as below:

$$Re = \frac{\dot{m} D_h}{\mu H W_{\mathrm{ch}}} \quad (2)$$

where $\dot{m}$, μ, and D_h are mass flow rate inside the channel, air viscosity, and channel hydraulic diameter, respectively. The Reynolds numbers range from 992 to 1722. Fig. 3 compares Nusselt numbers obtained from experiments and CFD. As expected, the Nusselt numbers monotonically become larger by increase in the mass flow rate and, in turn, Reynolds number. The excellent agreements (difference less than 6.1%) between computational and experimental Nusselt numbers indicate the accuracy of the simulation in this study.

The interactions of flow over perforations, particularly when the number of perorations increases, result in complex three-dimensional flow patterns that are challenging to be characterised through experiments because of requirement for sophisticated and costly visualization techniques. The validated and accurate simulation in this study is a beneficial to investigate the complex flow field over perforations. As the supplement to the present study, further research should be

performed to verify the temperature distribution across the heat sink base by simulating the flow and heat transfer over the entire heat sink (i.e., 19 channels). Also, higher Reynolds numbers should be investigated through accurate turbulence models. When sufficient understanding about thermo-fluid mechanisms in perforated fins is obtained, leveraging optimization techniques is essential to enhance heat transfer rate from perforated fins using input design parameters mainly perforation size, the distance between perforations, and configuration of perforations (inline or staggered). The simulation in the present study will be continued through future research to address some of the identified gaps.

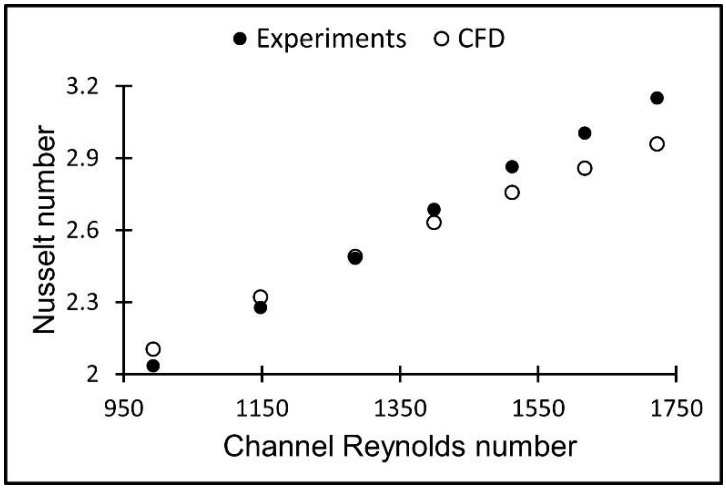

Fig. 3: Comparison of computational (CFD) and experimental Nusselt numbers in the perforated fin investigated in this study.

4. Conclusion

Three-dimensional simulation of forced convection heat transfer over a perforated fin was performed to obtain a validated simulation for predicting average heat transfer coefficients in perforated fins. Flow was laminar with maximum Reynolds number below 1722. Excellent agreements were obtained between computational and experimental Nusselt numbers. The validated numerical approach in the present study will be extended through future research to understand complex flow patterns over perforations and eventually develop optimized heat sinks made by perforated fins for enhancement of heat transfer rate.

Acknowledgements

This research is supported by the National Science Foundation-CREST Award (Contract # HRD-1914751) and the Department of Energy/National Nuclear Security Agency (DE-FOA-0003945).

References

[1] M.R. Shaeri, R. Bonner, "Heat transfer and pressure drop in laterally perforated-finned heat sinks across different flow regimes," *Int. Commun. Heat Mass Transfer*, vol. 87, pp. 220-227, 2017.

[2] B. Kanargi, P.S. Lee, C. Yap, "A numerical and experimental investigation of heat transfer and fluid flow characteristics of an air-cooled oblique-finned heat sink," *Int. J. Heat Mass Transfer*, vol. 116, pp. 393-416, 2018.

[3] V. Karlapalem, S.K. Dash, "Design of perforated branching fins in laminar natural convection," *Int. Commun. Heat Mass Transfer*, vol. 120, pp. 105071, 2021.

[4] M.R. Shaeri, R. Bonner, "Laminar forced convection heat transfer from laterally perforated-finned heat sinks," *Appl. Therm. Eng.*, vol. 116, pp. 406-418, 2017.

[5] M.R. Shaeri, R.W. Bonner III, "Analytical heat transfer model for laterally perforated-finned heat sinks," *Int. J. Heat Mass Transfer*, vol. 131, pp. 1164-1173, 2019.

[6] P. Teertstra, M.M. Yovanovich, J.R. Culham, "Analytical forced convection modeling of plate fin heat sinks," *J. Electronics Manufacturing*, vol. 10, pp. 253-261, 2000.